IEICE TRANS. COMMUN., VOL.E90–B, NO.6 JUNE 2007

PAPER Special Section on 2nd Pan-Pacific EMC Joint Meeting –PPEMC'06–

Characterization and Performance of High-Frequency Pulse Transmission for Human Body Area Communications

Jianqing WANG[†a)], *Member and* **Yuji NISHIKAWA**[†], *Student Member*

SUMMARY With the rapid progress of electronic and information technology, an expectation for the realization of body area network (BAN) has risen. However, on-body transmission characteristics are greatly dependent on the frequency, and a high-speed transmission is difficult due to the remarkable signal attenuation at higher frequencies. In this study, we proposed a pulse transmission system with the frequencies at dozens of mega-hertzes. The system was based on an impulse radio (IR) scheme with bi-phase modulation. By using the frequency-dependent finite difference time domain (FD^{2}TD) method, we investigated the on-body transmission characteristics and derived a path loss expression. Based on the transmission characteristics, we also investigated the influences of white Gaussian noises and other narrow-band interferences on the communication link budget and bit error rate (BER) performance. The results have shown the feasibility of the proposed on-body IR communication system.

key words: *on-body transmission, transmission characteristics, Debye approximation, FD^{2}TD method, impulse radio, bit error rate performance, interference*

1. Introduction

Toward the realization of ubiquitous society, information will be accessible at our fingertips, whenever and wherever needed. To provide this rapid access to information, some communication devices have to be incorporated into our attire and bodies. As electronic devices become smaller, lower in power requirements, and less expensive, wireless networking these devices on the human body has become available. Such an body area network (BAN) can share information effectively, reduce functional redundancies, and allow new conveniences and services [1]–[3]. For instance, an on-body system can allow the data transfer for personal identification and settlement of accounts just by touching the receiver for a user wearing a communication device. It can also allow users to exchange electronic business cards by shaking hands. In these cases, the human body acts as a transmission channel [4], which is superior to wireless transmission from the point of view of information security and electromagnetic compatibility. However, the electric signals attenuate remarkably at high frequencies on the human body. This has limited the on-body systems to lower frequencies ($\leq$ 10 MHz) [5], [6]. In the low-frequency systems, a low-frequency carrier is generally used so modulation is done at the carrier frequency band.

In this study, we aim at the investigation of the feasibility of a high-frequency pulse transmission on the human body because a base-band pulse transmission may yield a higher data rate, a lower power requirement and a simpler structure of transmitter and receiver. We first investigated the transmission characteristics of a high-frequency pulse on the human body area, and then we proposed a system based on an impulse-radio (IR) scheme for the on-body area communication. During the analysis of the on-body transmission characteristics, we employed the frequency-dependent finite difference time domain (FD^{2}TD) method [7] in which the Debye approximation is used to represent the frequency-dependent dielectric properties of human tissue. With the FD^{2}TD method in conjunction with a simplified arm model, we obtained the on-body transmission characteristics in the frequency domain. Moreover, based on the transmission characteristics, we derived the bit error rate (BER) and link budget under Gaussian noises for the proposed system, and also clarified the influence of other narrow-band interferences on the on-body pulse transmission.

Manuscript received August 28, 2006.
Manuscript revised November 17, 2006.

[†]The authors are with the Graduate School of Engineering, Nagoya Institute of Technology, Nagoya-shi, 466-8555 Japan.
a) E-mail: wang@nitech.ac.jp

DOI: 10.1093/ietcom/e90–b.6.1344

2. Analysis Method

The time-domain Maxwell's equations used for the FDTD method are

$$\nabla \times E(t) = -\mu \frac{\partial H(t)}{\partial t} \tag{1}$$

$$\nabla \times H(t) = \frac{\partial D(t)}{\partial t} + J_0(t) \tag{2}$$

where the electric flux density D is related to the electric field E thought the complex permittivity of human body tissue. Under the assumption that the complex relative permittivity of a human tissue can be approximated by the Debye equation

$$\varepsilon_r(\omega) = \varepsilon_\infty + \chi(\omega) + \frac{\sigma_0}{j\omega\varepsilon_0} \tag{3}$$

where ε_0 is the permittivity of free space, ε_∞ is the relative permittivity at frequencies approaching to infinity, $\chi(\omega)$ is the frequency-domain susceptibility, and σ_0 is the static electric conductivity, we can relate its first and second terms to $D(\omega)$ and the third term to $J_0(\omega)$ because only the former two terms are due to the frequency dispersion of tissue. We therefore have

$$D(\omega) = \varepsilon_0 \left[\varepsilon_\infty + \chi(\omega)\right] E(\omega) \tag{4}$$

$$J_0(\omega) = \sigma_0 E(\omega). \tag{5}$$

Since Eqs. (1) and (2) are to be solved iteratively in the time-domain by using the FDTD method, we need to transfer Eqs. (4) and (5) into the time-domain. This can be realized by Fourier transform. We thus have

$$D(t) = \varepsilon_0 \varepsilon_\infty E(t) + \varepsilon_0 \chi(t) * E(t) \tag{6}$$

$$J_0(t) = \sigma_0 E(t) \tag{7}$$

where the symbol * denotes the convolution. Substituting Eqs. (6) and (7) into Eq. (2) we get

$$\begin{aligned} E^n = {} & \frac{\varepsilon_\infty - \sigma_0 \Delta t/2\varepsilon_0}{\varepsilon_\infty + \chi^0 + \sigma_0 \Delta t/2\varepsilon_0} E^{n-1} \\ & + \frac{1}{\varepsilon_\infty + \chi^0 + \sigma_0 \Delta t/2\varepsilon_0} \Phi^{n-1} \\ & + \frac{\Delta t/\varepsilon_0}{\varepsilon_\infty + \chi^0 + \sigma_0 \Delta t/2\varepsilon_0} \nabla \times H^{n-1/2} \end{aligned} \tag{8}$$

where Φ^{n-1} is given by

$$\Phi^{n-1} = E^{n-1} \Delta\chi^0 + \sum_{m=1}^{n-2} E^{n-1-m} \Delta\chi^m \tag{9}$$

where $\Delta\chi^m$ will be given in the next chapter.

The difference for the Debye approximation from [7] in this study is the introduction of the static conductivity σ_0 which is meaningful at the frequency band of the pulse to be transmitted for human body tissue. As for the magnetic field calculation in the FD^{2}TD method, no modification is needed because the human tissue is nonmagnetic material.

3. Modeling of Human Body and Transmitter/Receiver

Since in most cases the on-body communication is through fingertips to the outside, we employed a simplified human arm model. Figure 1 shows the human arm model with a transmitter and receiver. The transmitter and receiver structures were first introduced in [4] at 10 MHz. They were composed of a signal electrode and a ground electrode, respectively, as shown in Figs. 1(b) and (c). The choice of the same electrode structure as [4] was based on the finding, as shown later (in Fig. 5), that its performance almost did not change over our interested frequency band. We applied the pulse signal voltage at the feeding point between the signal electrode and the upper circuit board in the transmitter, and detected the voltage at the receiving point in the receiver. In order to get the on-body path loss as a function of distance, we changed the distance between the transmitter and the receiver from 8 cm to 32 cm at a spacing of 8 cm.

In the choice of the high-frequency pulse signal to be transmitted, we paid attention to the frequency band of dozens of mega-hertzes. This was based on the following three considerations: (1) to get a higher transmission speed (> 10 MHz); (2) to maintain an acceptable signal intensity because the attenuation become remarkable at higher frequencies; and (3) to avoid possible narrow-band interferences such as FM radios. Based on these considerations, we therefore determined to use a second derivative of Gaussian pulse (Pulse width: ≤ 40 ns) as the signal $s(t)$ to be transmitted, i.e.,

$$s(t) = \left[1 - 2\alpha(t - \tau_0)^2\right] e^{-\alpha(t-\tau_0)^2} \tag{10}$$

where $\alpha = (4.0/\tau_0)^2$, and τ_0 denotes a time shift of the pulse. Figure 2 shows the transmitted pulse signal in the time domain and its normalized power spectrum in the frequency domain. As can be seen, its frequency bandwidth of 10 dB attenuation is between 15 MHz and 60 MHz. With respect to the center frequency of 35 MHz, the ratio of the occupation bandwidth to the center frequency is larger than 0.2. In this sense, the pulse can be considered as a ultra wideband (UWB) signal according to the definitation by Federal

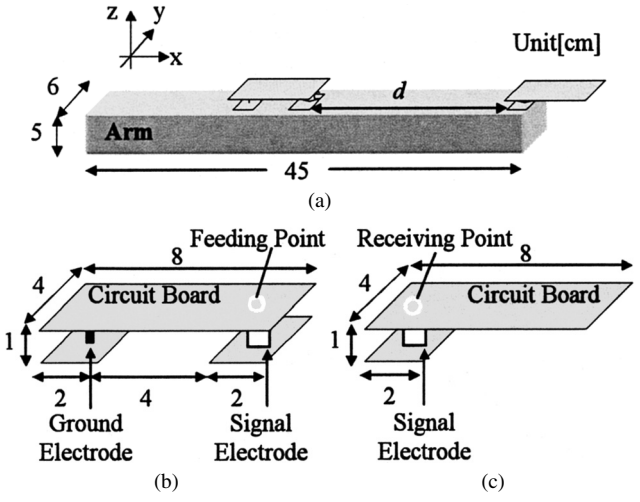

Fig. 1 Analysis model of on-body transmission. (a) Simplified human arm with transmitter and receiver, (b) enlargement of the transmitter structure, (c) enlargement of the receiver structure.

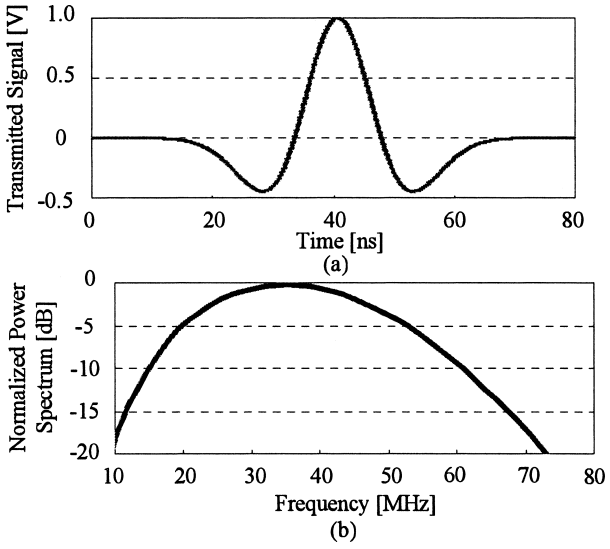

Fig. 2 (a) Pulse signal to be transmitted, (b) normalized power spectrum of the pulse.

Communications Commission (FCC) [8].

On the other hand, the arm was assumed as a homogeneous tissue, neither the skin nor the muscle. The complex relative permittivity of the arm model was determined by measurement. Figure 3 shows the measurement setup and measured data for four adults. The basic principle of the measurement setup is to derive the complex relative permittivity from measured S-parameters [9]. In view of the frequency band of the pulse to be transmitted, it is hard to consider that the arm acts as a waveguide. It seems to be a more reasonable explnantion that the signal is transmitted along the arm surface through electric field coupling. This is why we determined to measure the complex relative permittivity by probing the arm surface. However, due to the limitation of the employed dielectric probe at the interested frequency band, the measured data include some errors. To examine to what extent the measurement errors affect, we investigated the received pulse voltages for various complex relative permittivities assumed for the arm. They were the skin, muscle, 2/3-muscle, and so on. All of the complex relative permittivities were based on FCC recommendations. As a result, it was found that the received voltages calculated from the measured complex relative permittivity of arm was somewhat smaller, within 3 dB, than that calculated for the skin, muscle, or 2/3-muscle. This suggests that the employment of the measured complex relative permittivity has an acceptable accuracy, and actually it simulates a worst case transmission.

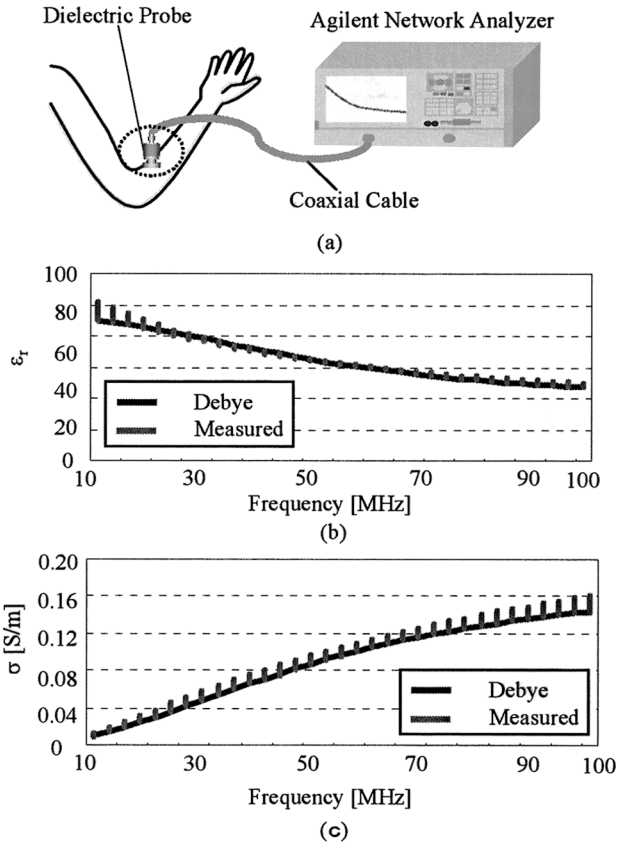

Fig. 3 Approximated and measured results of the complex relative permittivity of human arm. (a) Measurement setup, (b) $Re\{\varepsilon_r(\omega)\}$, and (c) $-\omega\varepsilon_0 Im\{\varepsilon_r(\omega)\}$.

To approximate the measured complex relative permittivity, we employed the one-relaxation Debye equation

$$\varepsilon_r(\omega) = \varepsilon_\infty + \frac{\varepsilon_s - \varepsilon_\infty}{1 + j\omega\tau} + \frac{\sigma_0}{j\omega\varepsilon_0} \tag{11}$$

where ε_s is the static relative permittivity, τ is the relaxation time and ω is the angular frequency. Based on the measured data, we obtained the parameters in Eq. (11) as $\epsilon_s = 92.12$, $\epsilon_\infty = 33.91$, $\tau = 1.5$ ns, and $\sigma_0 = 0.0053$ s/m in the sense of least square error. As can be seen from Figs. 3(b) and (c), the approximated complex relative permittivity agree well with the measurement in the interested frequency band.

From Eq. (11), it is easy to derive

$$\Delta\chi^m = (\varepsilon_s - \varepsilon_\infty)e^{-m\Delta t/\tau}\left(1 - e^{-\Delta t/\tau}\right)^2 \tag{12}$$

$$\Phi^{n-1} = E^{n-1}\Delta\chi^0 + e^{-\Delta t/\tau}\Phi^{n-2}. \tag{13}$$

This is known as the recursive convolution scheme as described in [7].

4. Transmission Characteristics

Using the FD^{2}TD method with a 5-mm voxel size, we calculated the on-body transmission characteristics (both the magnitude and phase) from the following equation

$$H(f) = \frac{F\{r(t)\}}{F\{s(t)\}} = |H(f)|\, e^{j\phi(f)} \tag{14}$$

where $s(t)$ is the transmitted pulse voltage at the feeding point of the transmitter, $r(t)$ is the received pulse voltage at the receiveing point of the receiver, and F denotes the Fourier transform. The group delay $D(f)$ was derived from

$$D(f) = -\frac{1}{2\pi}\frac{d\phi(f)}{df}. \tag{15}$$

Figure 4 shows the received pulse voltages at various distances between the transmitter and receiver in the time domain, and Fig. 5 shows the magnitude and group delay characteristics of the on-body transmission in the frequency domain. It was found that the magnitude of the transfer function $H(f)$ was almost smooth over the entire used frequency band although the received voltage decreased as the distance increased. The signal attenuation was about 17 dB at a distance of $d = 8$ cm. On the other hand, the group delay $D(f)$ increased roughly in proportion to the distance, especially between 30 MHz and 40 MHz. It ranged from 0.4 ns to 1.0 ns at 35 MHz for different distances but approached to 0.4–0.6 ns at frequencies higher than 40 MHz.

Based on the transmission characteristics, we derived an on-body path loss model for the high-frequency pulse transmission. The path loss was defined as the ratio of the transmitted pulse energy to the received pulse energy in unit of dB. According to an empirical power decay law [10], we

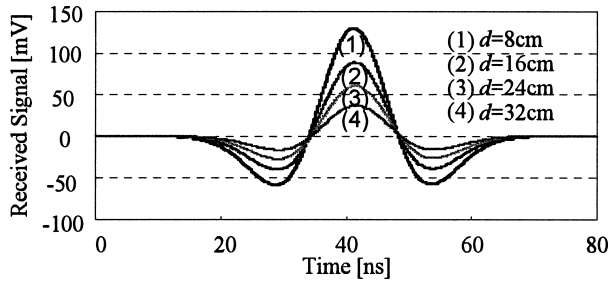

Fig. 4 Received pulse voltages at different transmitter/receiver distances.

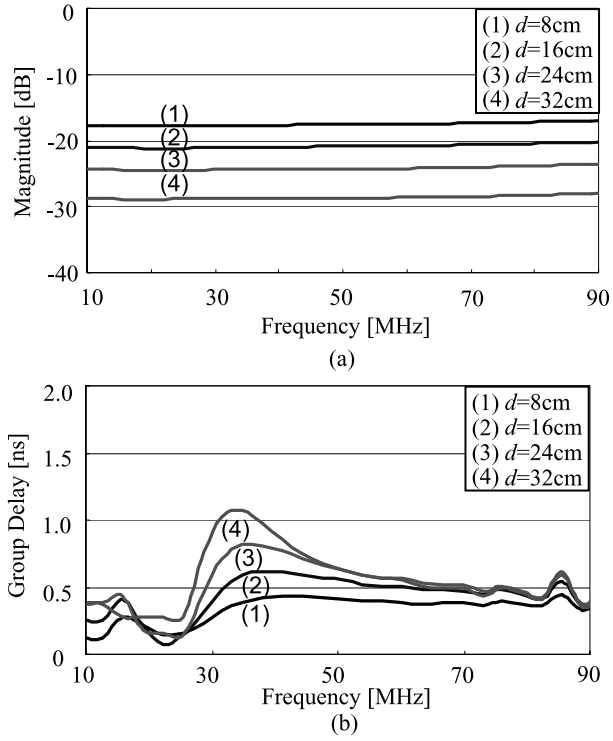

Fig. 5 On-body transmission characteristics in the frequency domain. (a) Magnitude, (b) group delay.

express the on-body path loss as

$$PL = PL_0 + 10n\log_{10}\left(\frac{d}{d_0}\right) \tag{16}$$

where PL_0 is the reference path loss at distance d_0, and n is the path loss exponent. By fitting this equation with the results in Fig. 4 in the sense of least square errors, we obtained the on-body path loss exponent of $n = 1.5$. This value is better than the free-space transmission because in that case the path loss exponent is known as 2.0. This finding means that the human body indeed acts as a transmission channel for the high-frequency pulse.

5. On-Body System Performance

Based on the on-body transmission characteristics, we proposed a base-band IR system for the on-body communication. Figure 6 shows the block diagram of the on-body IR

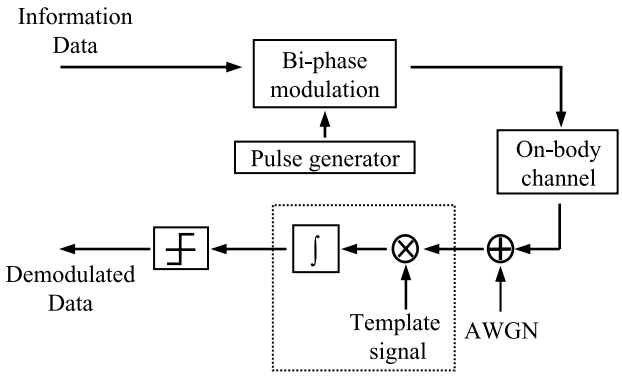

Fig. 6 Block diagram of the on-body impulse radio system.

system. The information data were modulated by bi-phase modulation and then transmitted via the antenna as a pulse train. After the on-body channel, the input $v_r(t)$ to the demodulator at the receiver is $r(t)$ plus the Gaussian noise $n(t)$. The receiver consisted of a pulse detector and a 1/0 decision circuit. The received signal was multiplied by a template signal and then their product was integrated, which was in reality a correlation detector. The BER of the system under Gaussian noises can be derived as

$$BER = \frac{1}{2}erfc\left(\sqrt{\frac{E_b}{N_0}\frac{\left[\int_0^{T_s} r(t)v_p(t)dt\right]^2}{\int_0^{T_s} r^2(t)dt\int_0^{T_s} v_p^2(t)dt}}\right) \tag{17}$$

where erfc is the complementary error function defined as

$$erfc(x) = 1 - \frac{2}{\sqrt{\pi}}\int_0^x \exp(-t^2)dt, \tag{18}$$

E_b is the received energy per bit, N_0 is the noise power spectral density, T_s is the pulse repetition period, and $v_p(t)$ is the template signal voltage. In this study we assumed it to be the transmitted voltage, i.e., $v_p(t) = s(t)$. In Eq. (17), if the pulse repetition period T_s is long enough, the term except for E_b/N_0 in the root is actually equal to the square of the correlation coefficient ρ. As shown in Fig. 4, the on-body channel resulted in a slight distortion of waveform, which would yield a correlation coefficient smaller than 1.0. In fact, the correlation coefficient was found to be around 0.99 for all the four received pulses in Fig. 4.

The performance of the propoesd on-body system was investigated by computer simulation, in which the FDTD-simulated on-body channel characteristics were employed. In Fig. 6, the bi-phase modulated pulses were the same as Fig. 2(a) or its reverse. After the on-body channel, the input signals to the receiver were the FDTD-calculated pulses as shown in Fig. 4. With the addition of white Gaussian noises (AWGN), the FDTD-calculated receiving pulses were input to the correlation detector. The operation of the correlation detector was performed by numerical calculation, and the 1/0 decision was based on the numerical intergation results in the correlation detector. The simulation code was written

in Matlab and validated to give the same BER performance as Eq. (17).

5.1 Influence of Gaussian Noise

For the proposed on-body system, we first investigated the BER and link budget under Gaussian noises. We assumed that the only noise source at the receiver is the white Gaussian noise. This noise is typically thermal, introduced by the circuitry of the receiver. The thermal noise power spectral density N_0 is given as

$$N_0 = kTN_F \tag{19}$$

where k is the Boltzman constant, T is the spot noise temperature, and N_F is the noise figure.

On the other hand, we assumed a peak voltage of 1 V for the transmitted pulse, which was similar to the carrier signal level in the literature [4]. In order to get the energy per bit E_b of the received pulse signal $r(t)$, we transformed $r(t)$ to the frequency domain $R(f)$ by the fast Fourier transform (FFT) and then calculated E_b from the integral of $Re\{R(f)R^*(f)/Z(f)\}$ in the frequency domain where $Z(f)$ is the input impedance at the receiver. We then can define a system margin M_s by

$$M_s = \frac{E_b/N_0}{[E_b/N_0]_{spec}} \tag{20}$$

where $[E_b/N_0]_{spec}$ denotes the E_b/N_0 level for obtaining an BER of 10^{-4}. According to Eq. (17), such an E_b/N_0 is about 8.5 dB.

Figure 7 shows the dependence of the system margin on the distance under the condition of a typical noise figure of $N_F = 10$ dB and a noise temperature of 27°C at the receiver. It was found that the system has a margin of nearly 30 dB for the thermal Gaussian noise even at a distance of 30 cm between the transmitter and receiver. It seems to be sufficiently feasible to secure a communication performance at the receiver from the thermal noises.

5.2 Influence of Narrow-Band Interference Signals

As shown in Fig. 2(b), most of the energy of the transmitted pulse was between 15 and 60 MHz. However, at this frequency band, amateur radios are a potential interference source to the on-body pulse transmission. In addition, FM radios may also interfere the on-body transmission because they have a carrier frequency close to the used frequency band. To investigate the influence of the narrow-band interferences, we considered two cases. One was the amateur radio at 29 MHz, and another was the FM radio at 76 MHz. The latter was not within the frequency band of 10 dB attenuation of the transmitted pulse. However, as can be seen from Fig. 2, that frequency component in the transmitted pulse was not zero because the attenuation was only about 20 dB. If the FM interference signal was large enough, it was still possible to distort the transmitted pulse waveform and therefore decrease the BER performance.

We assumed the received signal $v_r(t)$ with a narrow-band interference as

$$v_r(t) = Ar(t) + B\sin(2\pi ft + \theta) \tag{21}$$

where A is the received pulse peak voltage, B is the amplitude of narrow-band interference, f is the interference frequency, and θ is the phase difference from the transmitted pulse. Figure 8 shows the correlation coefficients of the received signal with the narrow-band interferences at 29 MHz and 76 MHz, respectively, as a function of the ratio of signal energy to interference energy (SIR) for different phase difference θ. An SIR of 10 dB corresponds to an $A/B \approx 6$. At 29 MHz, it was found that the worst case for the correlation coefficient was for a phase difference of π. When SIR

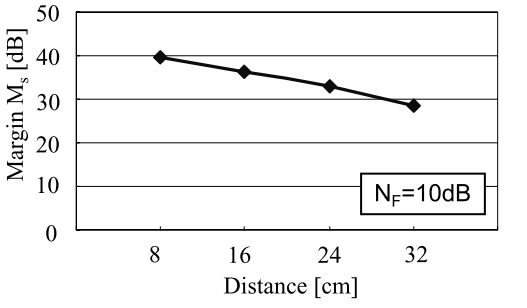

Fig. 7 Dependence of system margin M_s on the distance between the transmitter and receiver.

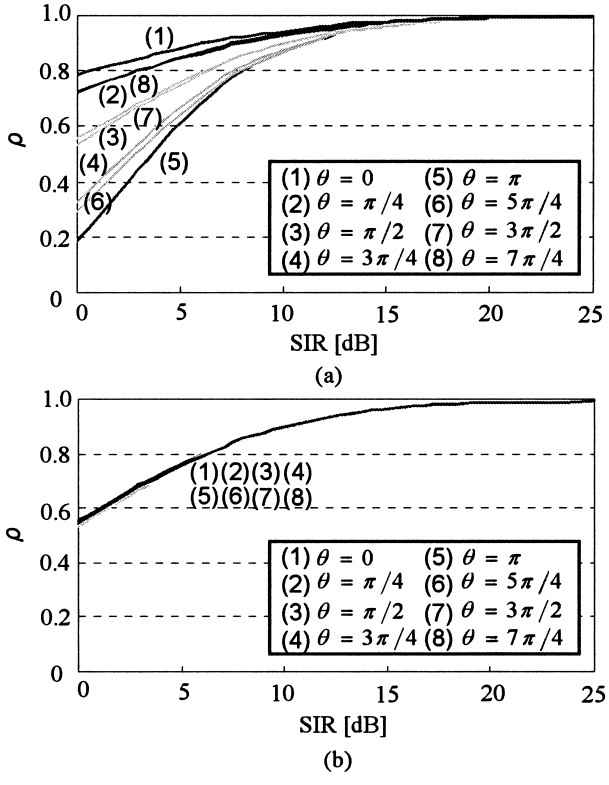

Fig. 8 Correlation coefficients versus SIR for different phase differences. (a) 29 MHz, (b) 76 MHz.

was larger than 10, however, the correlation coefficient was always larger than 0.9. On the other hand, at 76 MHz, it was found that an SIR of 10 or larger still gave a correlation coefficients larger than 0.9. Moreover, the correlation coefficient almost did not depend on the phase difference at 76 MHz. This can be explained from the fact that more sine periods were included in the received pulse period at 76 MHz so that the phase effect became insignificant.

As described in Eq. (17), the correlation coefficient is directly related to the BER. Figure 9 shows the BER as a function of SIR when $E_b/N_0 = 10$ dB. In each graph in Fig. 9, we plotted two BER curves. One was obtained from the phase difference θ where we had the best correlation coefficient, and another was for the phase difference θ where we had the worst correlation coefficient. The actual BER performance should be between the two curves, depending on the phase difference between the desired signal and the interference. From Fig. 9, it was found that at the both frequencies an SIR of 10 dB would give an BER smaller than 10^{-4}.

For a plane-wave incidence at the used frequency band, we also calculated the interference voltage induced at the receiver by using the FDTD method. It was found that for a 1 V/m (120 dBμV/m) plane-wave incidence the induced interference voltage has an amplitude of 23 mV, i.e., $B = 23$ mV in Eq. (20). In view of that the actual field intensity of the amateur radios and FM radios should be smaller than 1 V/m in most cases, an SIR larger than 10 dB ($A/B > 6$) should be an achievable quantity.

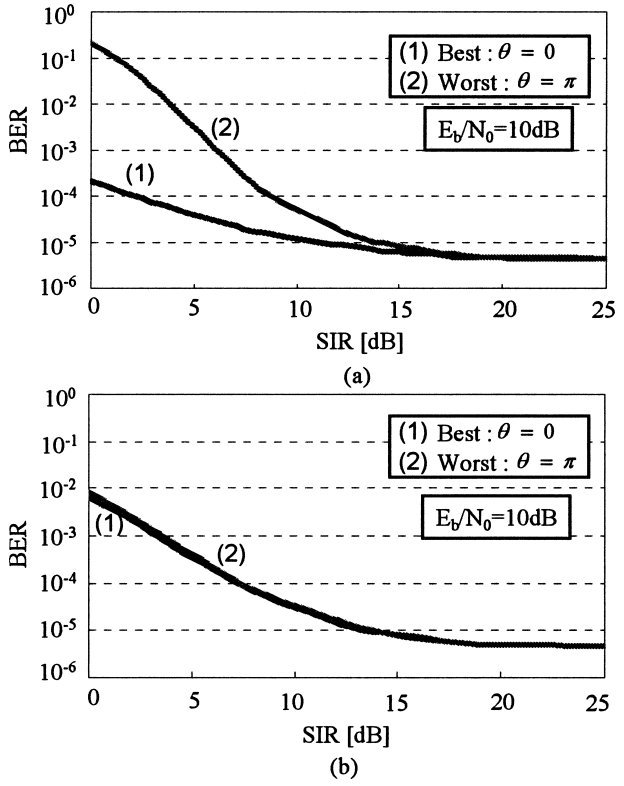

Fig. 9 BER performance versus SIR. (a) 29 MHz, (b) 76 MHz.

6. Conclusion

On-body area communications are essential in an ubiquitous society. In order to realize a high-speed on-body communication, in this study, we have proposed a pulse transmission system at dozens of mega-hertzes. The system is based on the IR scheme with bi-phase modulation. By using the FD^{2}TD method with a simplified human arm model, we have investigated the on-body transmission characteristics based on the measured human body properties. As a result, we have found a path loss exponent of $n = 1.5$ on the human body area. The smaller path loss exponent has implified a better on-body transmission compared to the case in free-space because in that case $n = 2$. Furthermore, based on the transmission characteristics, we have derived the BER performance under Gaussian noises for this system and also investigated the influence of narrow-band interference signals such as amateur radios and FM radios. The results have shown that an SIR of 10 dB can ensure an BER smaller than 10^{-4}.

Through the fundamental investigations, we have shown the feasibility of the proposed on-body communication system. The future subject is the circuitry design and experimental validation of this system.

Acknowledgement

This study was supported in part by Japan Society for the Promotion of Science (No.17560337).

References

[1] T.G. Zimmerman, "Personal area networks: Near-field intrabody communications," IBM Syst. J., vol.35, nos. 3&4, pp.609–617, 1996.
[2] http://grouper.ieee.org/groups/802/15/pub/Subscribe.html (IEEE 80 2.15 BAN).
[3] S. Matsuda, H. Harada, and R. Kohno, "A study on stochastic radiowave propagation model inside a human body," IEICE Technical Report, WBS2005-59, Dec. 2005.
[4] K. Fujii, M. Takahashi, K. Ito, K. Hachisuka, Y. Terauchi, Y. Kishi, K. Sasaki, and K. Itao, "Study on the transmission mechanism for wearable device using the human body as a transmission channel," IEICE Trans. Commun., vol.E88-B, no.6, pp.2401–2409, June 2005.
[5] M. Shinagawa, M. Fukumoto, K. Ochiai, and H. Kyuragi, "A near-field-sensing transceiver for intrabody communication based on the electrooptic effect," IEEE Trans. Instrum. Meas., vol.53, no.6, pp.1533–1538, Dec. 2004.
[6] M. Wegmuller, A. Lehner, J. Frohlich, R. Reutemann, M. Oberle, N. Felber, N. Kuster, O. Hess, and W. Fichtner, "Measurement system for the characterization of the human body as a communication channel at low frequency," Proc. 27th Annual International Conf. of IEEE Eng. in Med. Biol. Society, Shanghai, China, Sept. 2005.
[7] K.S. Kunz and R. Luebbers, The finite difference time domain method for electromagnetics, CRC Press, Boca Raton, 1993.
[8] M.-G. Di Benedetto and G. Giancola, Understanding ultra wide band radio fundamentals, Prentice Hall PTR, New Jersey, 2004.
[9] D. Misra, M. Chabbra, B.R. Epstein, M. Mirotznik, and K.R. Foster, "Noninvasive electrical characterization of materials at microwave frequencies using an open-ended coaxial line," IEEE Trans. Microw. Theory Tech., vol.38, no.1, pp.8–14, Jan. 1990.

[10] A. Fort, C. Desset, P. De Doncker, P. Wambacq, and L. Van Biesen, "An ultra-wideband body area propagation channel model — From statistics to implementation," IEEE Trans. Microw. Theory Tech., vol.54, no.4, pp.1820–1826, April 2006.

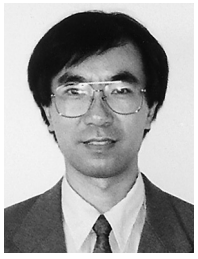

Jianqing Wang received the B.E. degree in electronic engineering from Beijing Institute of Technology, Beijing, China, in 1984, and the M.E. and D.E. degrees in electrical and communication engineering from Tohoku University, Sendai, Japan, in 1988 and 1991, respectively. He was a Research Associate at Tohoku University and a Senior Engineer at Sophia Systems Co., Ltd., prior to joining the Nagoya Institute of Technology, Nagoya, Japan, in 1997, where he is currently a Professor. His research interests include biomedical communications and electromagnetic compatibility.

Yuji Nishikawa received the B.E. degree in electrical and computer engineering from Nagoya Institute of Technology, Nagoya, Japan, in 2005. He is currently engaged in the study of intra and on-body area communications towards the M.E. degree.